Fluorescence properties of amido-substituted 2,3-naphthalimides: Excited-state intramolecular proton transfer (ESIPT) fluorescence and responses to Ca^{2+} ions

Lei Wang[a], Mayu Fujii[a], Misa Namba[a], Minoru Yamaji[b], Hideki Okamoto[a,] *

[a] *Division of Earth, Life, and Molecular Sciences, Graduate School of Natural Science and Technology, Okayama University, Tsushima-Naka 3-1-1, Kita-ku, Okayama 700-8530, Japan*
[b] *Division of Molecular Science, Graduate School of Science and Engineering, Gunma University, Ota, Gunma 373-0057, Japan*

ARTICLE INFO

Article history:
Received
Received in revised form
Accepted
Available online

Keywords:
Fluorescence
ESIPT
Naphthalimide
Ca^{2+} probe

ABSTRACT

Type your Abstract text here

2,3-Naphthalimide derivatives incorporating trifluoroacetamido (**3a**) and methansulfonamido (**3b**) functionalities at the 1-position were prepared and their intramolecular excited state proton transfer (ESIPT) fluorescence and responses to metal ions were investigated. Compound **3a** displayed normal fluorescence in the amide form in toluene and MeCN and no response to metal cations in the corresponding amidate ion form. In contrast, compound **3b** gave off dual emission assignable to normal and ESIPT fluorescence. Additionally, the amidate form of compound **3b** displayed off-on fluorescence response to Ca^{2+}.

Multifunctional fluorophores responding toward various external stimuli have been extensively investigated because of their potential applications to chemical sensors, analytical tools, bioprobes as well as lighting devices.[1–5] Excited state intramolecular proton transfer (ESIPT) is a widely studied photochemical process in which an acidic proton in an excited normal-form chromophore **N*** intramolecularly migrates to the hydrogen-bonded acceptor atom to produce the corresponding excited state tautomer **T*** (Figure 1).[6] Representatively, the hydrogen donor is a hydroxy group. The excited tautomer **T*** will return to its ground state **T** followed by thermal ground-state intramolecular proton transfer (GSIPT) to reproduce the original chromophore **N**. Fluorescence emission given off through an ESIPT process displays huge Stokes shift as large as 6000–12000 cm^{-1}, because **T*** is lower in energy than initially formed **N***, and **T** is higher in state energy than the original chromophore **N** in the ground state.[7]

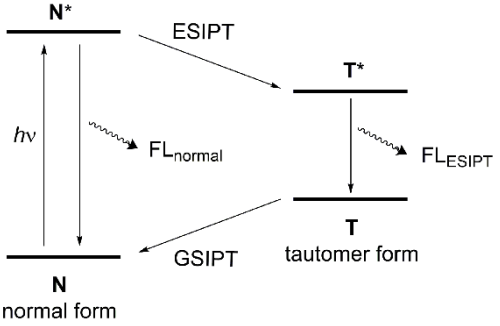

Figure 1. Schematic diagram for an ESIPT cycle.

ESIPT fluorescence is affected by various external stimuli such as solvent polarity, intramolecular and intermolecular hydrogen bonding, pH, and ionic species.[8,9] Accordingly, ESIPT fluorophores are expected to serve as multifunctional fluorescent probes.[10–12] Additionally, as dual fluorescence is often observed from **N*** (FL_{normal}) and **T*** (FL_{ESIPT}), ESIPT fluorophores can be used as a single-molecule white-light emitter through fine tuning of FL_{normal} and FL_{ESIPT} ratio.[13]

Most conventional ESIPT fluorophores, represented by 2-(2'-hydrohyphenyl)-substituted benzimidazoles (HBI),[14] bonzoxazoles (HBO),[15] and benzothiazoles (HBT),[16] have hydroxy group as the proton donor (OH type). In contrast, ESIPT fluorophores possessing proton donor of amino- or amido functionalities (NH type) have been less investigated. The pioneering system of NH type ESIPT was based on trifluoroacetamide derivative of 9,10-anthraquinone.[17] Later, the detailed amido-substituent effects on the ESIPT fluorescence behavior of the 9,10-anthraquinone derivatives were studied and analyzed by the nodal-plane model.[18] Because nitrogen atom has three valences, one can utilize the third substituent to modify NH type ESIPT behavior without changing the chromophore structure and the strategy was recently reviewed.[19]

It would be of an additional interest that, as the migrating O-H and N-H protons in ESIPT fluorophores are acidic, they can be easily removed with an appropriate base to generate the corresponding enolate/amidate form ($\mathbf{E}^-$) (Scheme 1a). The anionic form $\mathbf{E}^-$ has a bidentate electron-pair donating structure. Such a chelating structure has been used for metal ion binding. Thus, it was reported that water soluble HBI, HBO, and HBT derivatives bound with Zn^{2+} to form **E**-Zn complex in an aqueous

medium,[20] and a modified HBO derivative selectively formed a complex with Li^+ (**E**-Li) in organic media in the presence of a base.[21]

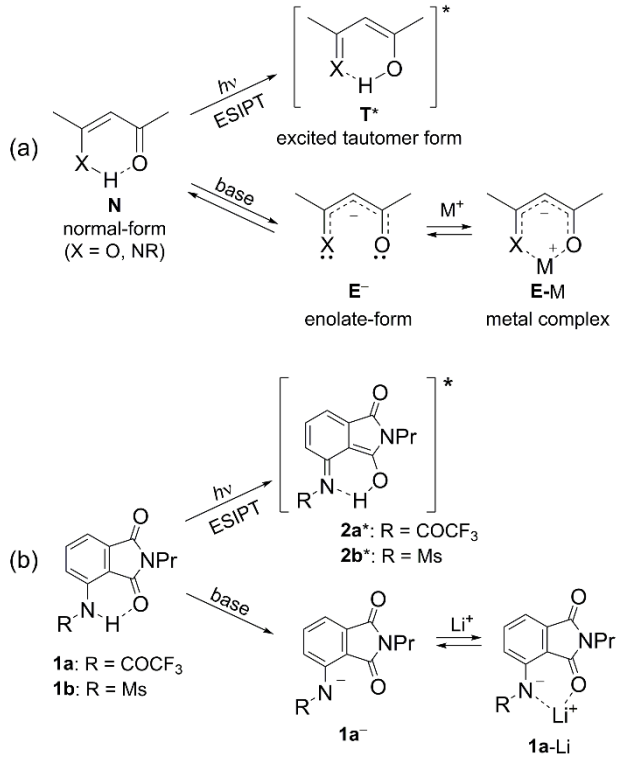

Scheme 1. Modification of ESIPT fluorescence behavior: (a) general concept, (b) fluorescence modification of phthalimide-based N-H type ESIPT.

NH-type ESIPT fluorescer with an imide proton-acceptor is rather rare. The present authors reported that trifluoroacetamide (TfAc-amide) and methanesulfonamide (Ms-amide) derivatives of phthalimide, **1a** and **1b**, efficiently produce ESIPT fluorescence from the corresponding excited tautomer **2*** and the fluorescence color can be tuned by the amido substituents without changing the phthalimide core.[22,23] Additionally, the amidate form $\mathbf{1a}^-$ selectively bound to Li^+ to show enhanced blue fluorescence from **1a**-Li.[22] Based on the fluorescence color changes among **1a**, $\mathbf{1a}^-$, and **1a**-Li, this simple compound serves as a potential multifunctional fluorescent probe.

These observations on phthalimide **1** promoted us to investigate fluorescence behavior of π-extended homologues **3a** and **3b** (See structures for Figure 2), because it was expected that these compounds would show modified fluorescence behavior compared to compounds **1a** and **1b** due to the difference in electronic features. Additionally, as naphthalimides **3** have a peri-hydrogen atom at the C8 position, it would sterically interact with the amido functionalities to modulate the fluorescence behavior. Herein, we report ESIPT fluorescence spectral features of TfAc-amide **3a** and Ms-amide **3b** and their responses to metal ions in the presence of a base in MeCN.

Figure 2. Chemical structures of amido-substituted naphthalimides **3** and the corresponding amidates $\mathbf{3}^-$ and tautomers **4**.

Synthesis and characterization of new compounds are described in Supplementary Information. Absorption and fluorescence spectra of compounds **3a** and **3b** were measured in toluene (none polar), MeCN (polar), and DMSO (polar and proton accepting) to understand their electronic features (Figure 3) and the photophysical parameters are collected in Table 1. In toluene and MeCN, compounds **3a** and **3b** showed a structured absorption band at around λ^{Abs}_{max} 360 and 366 nm (log ε = 3.6), respectively. The differences of the amido functionalities only slightly affected their absorption properties. In toluene and MeCN, TfAc-amide **3a** displayed emission band at λ^{FL}_{max} *ca*. 415 nm. Considering the Stokes shift values (3510–3680 cm^{-1}), the emission bands are assigned to normal fluorescence from the amide form. In DMSO, TfAc-amide **3a** showed a red-shifted absorption band (λ^{Abs}_{max} 367 nm) accompanied by a red-shifted fluorescence band at λ^{FL}_{max} 506 nm. The spectral profiles were similar to those of amidate $\mathbf{3a}^-$, which was generated in MeCN by addition of 1,8-diazabicyclo[5.4.0]undec-7-ene (DBU) (Figure S1). The 506-nm emission band in DMSO was assigned not to tautomer **4a*** but to amidate $\mathbf{3a}^-$. Thus, different from the case of phthalimide **1a**, the higher homologue **3a** does not undergo ESIPT process.[22,23]

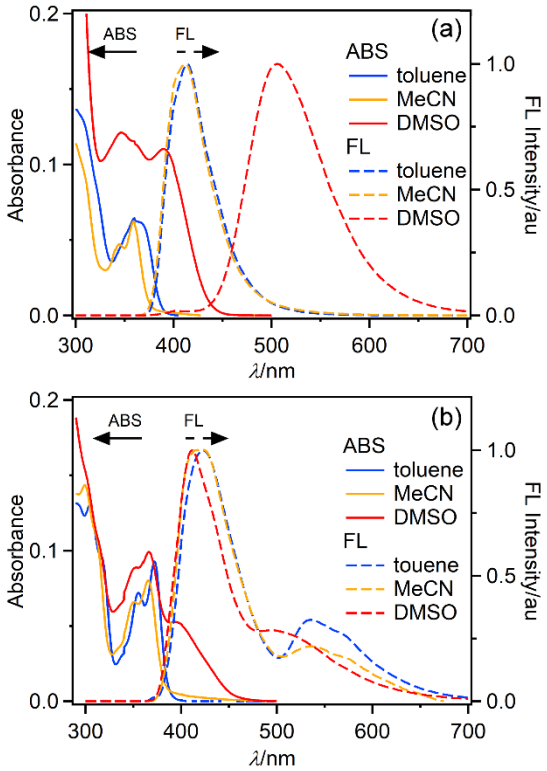

Figure 3. Absorption and fluorescence spectra of compounds **3a** (a) and **3b** (b).

Ms-amide **3b** gave off dual emission in the above mentioned three solvents (Figure 3b). In toluene, fluorescence bands were observed at λ^{FL}_{max} 423 and 538 nm. By considering the Stokes shift, these two emission bands were respectively assigned to normal emission from **3b*** and ESIPT emission from tautomer **4b***. These results were supported by the fact that the excitation spectra of the two emission bands were identical with the absorption spectra of **3b** (Figure S2). In MeCN, Ms-amide **3b** also displayed normal and ESIPT fluorescence. In DMSO, Ms-amide **3b** displayed a shoulder absorption band at around 400 nm in addition to an absorption band at 370 nm, and emitted dual fluorescence at λ^{FL}_{max} 411 and 511 nm. The excitation spectra for the two fluorescence bands were different from each other and that for the 511-nm band was similar with the absorption spectrum of the corresponding amidate $\mathbf{3b}^-$ generated by addition of DBU in MeCN (Figures S2 and S3). Thus, the 511-nm emission band was assigned to amidate form $\mathbf{3b}^-$

formed though spontaneous deprotonation in DMSO in the ground state.

Table 1. Photophysical parameters of compounds **3a** and **3b**[a]

Compound	Solvent	λ^{Abs}_{max} /nm (log ε)	λ^{FL}_{max} /nm (Φ_F)[b]	Stokes shift/cm^{-1}
3a	Toluene	360 (3.51)	415	3680
	MeCN	360 (3.58)	412 (0.18)	3510
	DMSO	397[c]	506	5430
	Solid state	—	401, 430	—
3b	Toluene	372 (3.67)	423, 538	3240[d], 8290[e]
	MeCN	366 (3.62)	422, 534 (0.01)	3680[d], 8740[e]
	DMSO	368, 397[c]	411, 511	2810[d], 5620[f]
	Solid state	—	417, 488	—

[a] Absorption and fluorescence spectra were measured at room temperature under aerobic conditions.
[b] Fluorescence quantum yields (Φ_F) were determined by using quinine sulfate (Φ_F = 0.55 in 0.1 M H_2SO_4) as the reference.[24]
[c] The ε values were not determined due to formation of the corresponding deprotonated forms **3**$^-$.
[d] For normal fluorescence.
[e] For ESIPT fluorescence.
[f] For amidate fluorescence.

Solid-state fluorescence of compounds **3a** and **3b** was measured because solid-state emitters are of an interest from the aspect of device applications.[12] Compounds **3a** and **3b** produced blue fluorescence in the solid state (Figure 4). TfAc-amide **3a** showed structured normal emission with λ^{FL}_{max} 430 nm whereas Ms-amide **3b** gave off dual fluorescence at λ^{FL}_{max} 417 (normal) and 488 (ESIPT) nm. The normal emission band located in the similar wavelength region as that in solution, by contrast, the solid state emission band appeared in the shorter wavelength region than that observed in solution (λ^{FL}_{max} 534 nm). It is presumed that the emitting tautomer structure **4b*** could not be relaxed into the most stable molecular structure because of the restricted motion in the solid state.

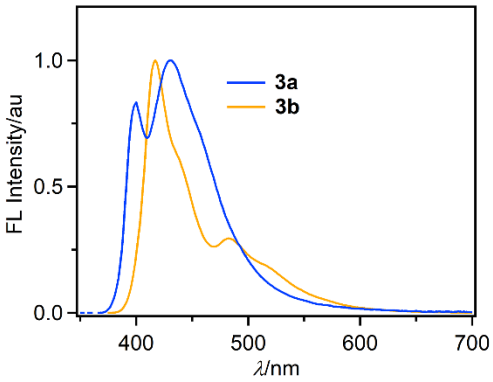

Figure 4. Fluorescence spectra of compounds **3a** and **3b** in the solid state.

To understand the difference in the ESIPT behavior between TfAc-amide **3a** and Ms-amide **3b**, the excited state energy profiles for the involved species were calculated by time-dependent density functional theory (TD-DFT)[25–27] at the PBE0/6-311+G(d,p) level.[28,29] Figure 5 shows the energy profiles with the calculated and experimental electronic transition wavelengths. After photoexcitation, the Franck-Condon structure **3a*** produces a relaxed structure **3a'*** within the excited-state lifetime. Because the conversion from **3a'*** to **4a*** is energetically uphill, the ESIPT process is predicted to be undesired. For Ms-amide **3b**, excited state **3b'*** and the tautomer **4b*** are calculated to be almost same in energy, thus, these two species are expected to be in an equilibrium within the excited-state lifetime. Thus, two emission bands from **3b'*** and **4b*** are reasonably expected, and the calculation results are consistent with the experimental observations; TfAc-amide **3a** showed no ESIPT fluorescence whereas Ms-amide **3b** displayed normal and ESIPT dual emission. The calculated results qualitatively support the experimental results.

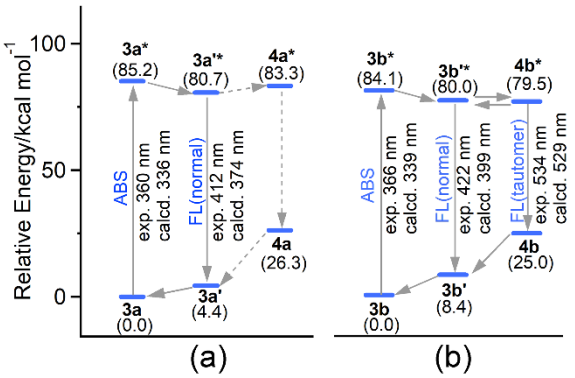

Figure 5. Calculated energy diagram for the ESIPT cycles of **3a** (a) and **3b** (b). **3a*** and **3b*** represent the Franck-Condon structures, and **3a'*** and **3b'*** denote relaxed structures in the S_1 state. Energies in the ground state (S_0) were calculated at the PBE0/6-311+G(d,p) level and geometries and the vertical electronic transition energies were estimated by the TD-PBE0/6-311+G(d,p) method. The processes occurred and those not occurred are respectively shown with full-line arrows and dotted-line arrows.

The optimized structure of excited tautomer **4a*** and **4b*** are illustrated in Figure 6. The torsion angle around the C1=N double bond was calculated to be ∠C8a-C1-N-C(=O) 33.8° for **4a*** and ∠C8a-C1-N-S 15.8° for **4b***. In the case of **4a***, C1=N bond is more significantly deviated from planarity than the case of **4b*** due to the steric repulsion between the trifluoroacetyl moiety and the peri-hydrogen atom on the C8 position. This steric effect is considered to be one of the factors to destabilize the excited state structure **4a*** resulting in the ESIPT process energetically unfavorable for TfAc-amide **3a**. On the other hand, excited tautomer **4b*** is considered to be more effectively stabilized by conjugation of the C1=N bond with the π system thus the energy level of exited tautomer **4a*** was lowered to make the ESIPT process possible.

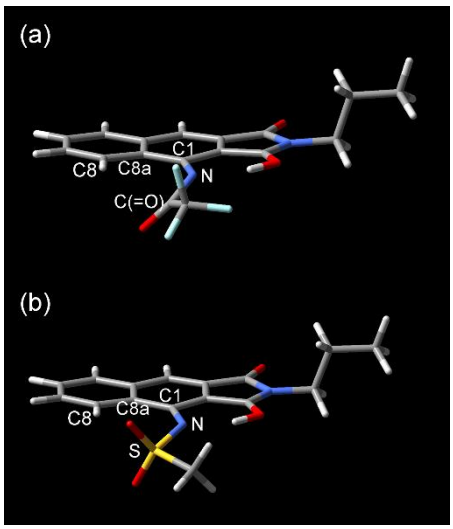

Figure 6. Calculated structures of tautomers **4a*** (a) and **4b*** (b) in S_1 state. The geometries were optimized by the TD-PBE0/6-311+G(d,p) method. ∠C8a–C1–N–C(=O) 33.8°, ∠C8a–C1–N–S 15.8°.

It has been reported that compound **1a** selectively responded to Li^+ in its amidate form to display modulated fluorescence behavior.[21] Because negatively charged amidates **3a**$^-$, **3b**$^-$ were expected to respond to metal ions as in the case of compound **1a**

(Scheme 1b), their fluorescence properties were investigated in the presence of metal ions in MeCN. The amidate **3a**$^-$ and **3b**$^-$ were generated by addition of 2–3 equiv. of DBU in MeCN (Figure S4) and the electronic spectra were observed after addition of 5 equiv. of metal salts (Figure 7). Amidate **3a**$^-$ displayed little changes in electronic spectra upon addition of alkali-metal ions (Figure 7a,b). Addition of alkali-earth metal ions and Zn^{2+} showed reproduction of protonated amide form **3a** through a metal ion induced hydrolysis.[30] Thus, amidate **3a**$^-$ underwent no specific binding with the metal ions. The results show clear contrast to the Li^+-selective binding of lower homologue **1a**$^-$.

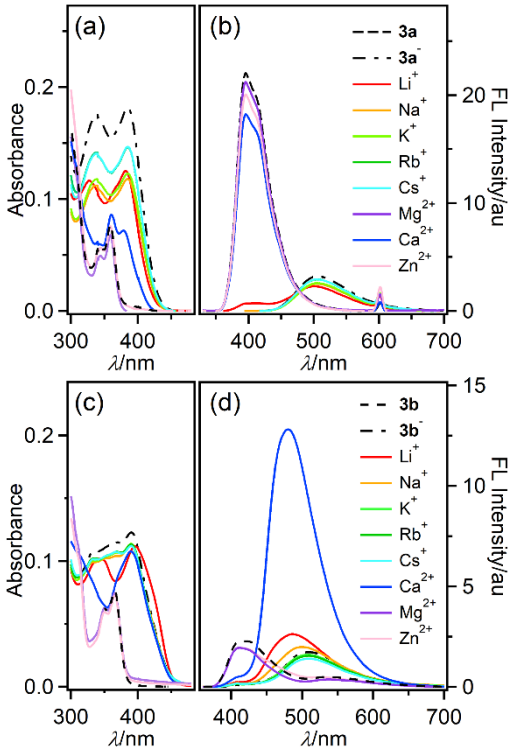

Figure 7. Absorption and fluorescence spectra of compounds **3a** (a,b) and **3b** (c,d) observed after addition of metal ions (5 equiv.) in the presence of DBU (2 equiv. for **3a**, 3 equiv. for **3b**) in MeCN. [**3a**], [**3b**] = 2×10^{-5} M.

In the case of amidate **3b**$^-$, alkali-metal ions other than Li^+ showed minimal effects on the absorption and fluorescence spectra, and Mg^{2+} and Zn^{2+} generated protonated form **3b** as in the case of **3a**$^-$ through the metal ion induced hydrolysis (Figure 7c,d). Addition of Li^+ induced new absorption bands at λ^{Abs}_{max} 396 and 344 nm, correspondingly, the fluorescence band blue shifted to λ^{FL}_{max} 486 nm compared to **3b**$^-$ (λ^{FL}_{max} 509 nm). Upon addition of Ca^{2+}, an absorption band appeared at λ^{Abs}_{max} 390 nm accompanied by enhanced fluorescence emission band at λ^{FL}_{max} 480 nm (Figure 7c,d). The fluorescence quantum yield Φ_F was determined to be 0.01 for **3b**$^-$ without an additive, 0.01 for **3b**$^-$ with Li^+, and 0.14 for **3b**$^-$ with Ca^{2+}. Therefore, amidate **3b**$^-$ responded to Li^+ and Ca^{2+} with a blue shift in the fluorescence band ($\Delta\lambda^{FL}_{max}$ −23 nm for Li^+, −29 nm for Ca^{2+}) and, namely, enhanced fluorescence intensity in the presence of Ca^{2+}. It is, thus, concluded that Ms-amide **3b** would serve as fluorescence off-on probe for Ca^{2+} ions in its amidate form **3b**$^-$. In DMSO, Ms-amide **3b** spontaneously dissociates in part to **3b**$^-$, however, the amidate form **3b**$^-$ did not show interaction with Ca^{2+} in DMSO (Figure S5). This is because that solvation of Ca^{2+} with DMSO molecules was predominant compared to interaction between **3b**$^-$ and Ca^{2+}. The Ca^{2+} adduct of **3b**$^-$ was isolated as a pale yellow solid and its composition was determined most likely to be **3b**$^-$$(CaOTf)^+$ based on its elemental analysis results (see experimental in SI). The counter ion ($^-$OTf) came from the counter anion of the Ca salt used ($Ca(OTf)_2$).

In summary, fluorescence behavior of amido-substituted naphthalimides **3a** and **3b** was revealed. TfAc-amide **3a** solely displayed normal fluorescence whereas Ms-amide **3b** gave off normal and ESIPT fluorescence. To the best of our knowledge, this is the first observation of NH-type ESIPT fluorescence with 2,3-naphthalimide chromophore. The difference of the ESIPT behavior was qualitatively understood by the theoretical calculation results, that the amido functionalities modified the energetic relationships between the excited state naphthalimides **3'*** and the corresponding tautomers **4***. Ms-amide **3b** selectively responded to Ca^{2+} with its amidate form **3b**$^-$ showing the blue shifted and enhanced fluorescence emission band at λ^{FL}_{max} 509 nm. Therefore, Ms-amide **3b** would serve as a multifunctional fluorophore.

Acknowledgments

The present study was partly supported by a Grant-in-aide for Scientific Research (KAKENHI) No. JP17K05976 and JP18H02043 from JSPS, and The Pre-collaboration support program of Okayama University. The authors thank the Micro Elemental Analysis Laboratory of Okayama University for the combustion analysis of the novel compounds.

References and notes

1. Jiménz-Sánchez, A.; Lei, E. K.; Kelley, S. O. *Angew. Chem. Int. Ed*. **2018**, *57*, 8891–8895.
2. Luo, J.; Uprety, R.; Naro, Y. Chou, C.; Nguyen, D. P.; Chin, J. W.; Deiters, A. *J. Am. Chem. Soc.* **2014**, *136*, 15551−15558.
3. He, L.; Yang, X.; Xu, K.; Yang, Y.; Lin, W. *Chem. Commun*. **2017**, *53*, 13168−13171.
4. Su, F.; Agarwal, S.; Pan, T.; Qiao, Y.; Zhang, L.; Shi, Z.; Kong, X.; Day, K.; Chen, M.; Meldrum, D.; Kodibagkar, V. D.; Tian. Y. *ACS Appl. Mater. Interfaces* **2018**, *10*, 1556−1565.
5. Weller, A. *Z. Elektrochem*. **1956**, *60*, 1144–1147.
6. Kwon, J. E.; Park, S. Y. *Adv. Mater*. **2011**, *23*, 3615–3642.
7. Tomin, V. I.; Demchenko, A. P.; Chou, P.-T. *J. Photochem. Photobiol. C*. **2015**, *22*, 1–18.
8. Demchenko, A. P.; Tang, K.-C.; Chou, P.-T. Chem. Soc. Rev., 2013, 42, 1379–1408.
9. Sedgwick, A. C.; Wu, L.; Han, H.-H.; Bull, S. D.; He, X.-P.; James, T. D.; Sessler, J. L.; Tang, B. Z.; Tian, H.; Yoon, J. *Chem. Soc. Rev.* **2018**, *47*, 8842–8880.
10. Zhao, J.; Ji, S.; Chen, Y.; Guo, H.; Yang, P. *Phys. Chem. Chem. Phys*. **2012**, *14*, 8803–8817.
11. Liu, Z.; He, W.; Guo, Z. *Chem. Soc. Rev*. **2013**, *42*, 1568–1600.
12. Padalkar, V. S.; Seki, S. *Chem. Soc. Rev*. **2016**, *45*, 169–202.
13. Massue, J.; Jacquemin, D.; Ulrich, G. *Chem. Lett*. **2018**, *47*, 1083–1089.
14. Sinha, H. K.; Dogra, S. K. *Chem. Phys*. **1986**, *102*, 337–347.
15. Mordziński, A.; Grabowska, A. *Chem. Phys. Lett*. **1982**, *90*, 122–127.
16. Cohen, M. D.; Flavian, S. *J. Chem. Soc. B*. **1967**, 317–321.
17. Smith, T. P.; Zaklika, K. A.; Thakur, K. B. P. F. *J. Am. Chem. Soc*. **1991**, *113*, 4035–4036.
18. Nagaoka, S.; Endo, H.; Ohara, K.; Nagashima, U. *J. Phys. Chem. B* **2015**, *119*, 2525−2532.
19. Chen, C.-L.; Chen, Y.-T.; Demchenko, A. P.; Chou, P.-T. *Nat. Rev. Chem*. **2018**, *2*, 131–143.
20. Henary, M. M.; Fahrni, C. J. *J. Phys. Chem. A* **2002**, *106*, 5210–5220.
21. Obare, S. O.; Murphy, C. J. *New J. Chem*. **2001**, *25*, 1600–1604.
22. Okamoto, H.; Konishi, H.; Satake, K. *Chem. Commun*. **2012**, *48*, 2346–2348.
23. Okamoto, H.; Itani, K.; Yamaji, M.; Konishi, H.; Ota, H. *Tetrahedron Lett*. **2018**, *59*, 388−391.
24. Melhuish, W. H. *J. Phys. Chem*. **1961**, *65*, 229–235.
25. Bauernschmitt, R.; Ahlrichs, R. *Chem. Phys. Lett*. **1996**, *256*, 454–464.
26. Stratmann, R. E.; Scuseria, G. E.; Frisch, M. J. *J. Chem. Phys*. **1998**, *109*, 8218−8224.
27. Casida, M. E.; Jamorski, C.; Casida, K. C.; Salahub, D. R. *J. Chem. Phys*. **1998**, *108*, 4439–4449.

28. Adamo, C.; Barone, V. *J. Chem. Phys*. **1999**, *110*, 6158–6170.
29. Krishnan, R.; Binkley, J. S.; Seeger, R.; Pople, J. A. *J. Chem. Phys.* **1980**, *72*, 650-654.
30. Takemura, H.; Nakashima, S.; Kon, N.; Yasutake, M.; Shinmyozu, T.; Inazu, T. *J. Am. Chem. Soc*. **2001**, *123*, 9293–9298.

Supplementary Material

Supplementary data associated with this article (experimental details, absorption and fluorescence excitation spectra, theoretical calculation results, NMR spectra of the new compounds) can be found in the online version.